Communications Biology

https://doi.org/10.1038/s42003-026-09794-6

Article in Press

The role of dorsal anterior cingulate cortex in dynamic attitude changes in naturalistic settings

Received: 26 September 2025

Accepted: 20 February 2026

Cite this article as: Li, H., Yao, S., Zhang, Y. *et al.* The role of dorsal anterior cingulate cortex in dynamic attitude changes in naturalistic settings. *Commun Biol* (2026). https://doi.org/10.1038/s42003-026-09794-6

Haiming Li, Senmu Yao, Yu Zhang, Bing Wu & Yi Liu

The Role of Dorsal Anterior Cingulate Cortex in Dynamic Attitude Changes in Naturalistic Settings

Haiming Li[1,2], Senmu Yao[3,4], Yu Zhang[1,2], Bing Wu[3,4]*, Yi Liu[1,2]*

[1]School of Psychology, Northeast Normal University, Changchun 130024, China

[2]Jilin Provincial Key Laboratory of Cognitive Neuroscience and Brain Development, Changchun 130024, China

[3]Chinese PLA Medical School, No. 28 Fuxing Road, Haidian District, Beijing 100853, China

[4]Department of Radiology, Seventh Medical Center of Chinese PLA General Hospital, No. 5 Nanmencang, Dongcheng District, Beijing 100700, China

*Corresponding author:

Yi Liu (liuy930@nenu.edu.cn), Northeast Normal University, Changchun 130024, Jilin, China.

Bing Wu (13910720619@163.com), Department of Radiology, Seventh Medical Center of Chinese PLA General Hospital, No. 5 Nanmencang, Dongcheng District, Beijing 100700, China.

Abstract

Attitudes change gradually and spontaneously in daily life, yet the neural mechanisms supporting such dynamic shifts remain poorly understood. Leveraging naturalistic fMRI paradigms across two studies, we investigated how neural dynamics track and implement attitude change during exposure to persuasive arguments. Our findings highlight the dorsal anterior cingulate cortex (dACC) as a central hub in this process. Individuals with more similar trajectories of attitude change exhibited greater similarity in the temporal dynamics of dACC activity and its functional connectivity with other brain regions, particularly the default mode network (DMN). These neural dynamics further predicted whether an individual changed their attitude over time, and at the precise moment of change, dACC-centered connectivity predicted the direction of that change. Additionally, individuals with higher intolerance of uncertainty (IU) showed stronger coupling between neural and behavioral similarity, suggesting that IU may serve as a trait-level modulator of this neural process. Together, our findings provide a dACC-centered, process-level account of the neural mechanisms underlying dynamic attitude change, bridging the gap between controlled laboratory research and real-time, naturalistic attitude change in daily life.

Keywords: attitude change, dorsal anterior cingulate cortex (dACC), neural dynamics, naturalistic paradigm

Introduction

In daily life, we often hold opinions on certain issues, but they are far from fixed. Our attitudes are frequently influenced by the deluge of persuasive information, causing us to swing back and forth between different positions. How the brain tracks the dynamic changes in attitude as we constantly receive persuasive information, and determines whether and how we change our minds, is an intriguing yet under-researched issue.

Looking at previous research on attitude changes, most studies measured one-shot attitude changes on a trial-by-trial basis[1–10]. One line of research induced attitude changes through social conformity[1–5] or cognitive dissonance[6–10] and consistently showed that activity in the dorsal anterior cingulate cortex (dACC) was associated with attitude change (see refs 11,12 for reviews). This involvement has typically been interpreted through the lens of conflict monitoring. That is, detecting discrepancies between personal beliefs and group norms, or between one's attitudes and behaviors. While influential, this perspective reflects only a narrow view of dACC function. A more integration view known as meta-reinforcement learning model proposed that prefrontal cortex including dACC serves as a meta-level controller, not merely detecting conflict, but dynamically guiding whether and how to adjust internal strategies in response to evolving environmental input[13–15]. This model is especially relevant for naturalistic attitude change, which requires ongoing integration of persuasive, often ambiguous information. If this is the case, the dACC should not only respond to one-shot attitude changes but also track dynamic fluctuations in attitude, and potentially signal whether and how a person changes their mind in real time. However, no empirical studies have directly tested this hypothesis to date.

Another line of research has examined attitude change in the context of health-related behaviors[16–21]. These studies have found that stronger activity in the ventromedial prefrontal cortex (vmPFC) and dorsomedial prefrontal cortex (dmPFC) during message processing predicts greater attitude/behavior changes related to drinking[16], smoking[17,18], sedentary behavior[19] and sunscreen use[20,21]. The vmPFC is thought to represent subjective value or personal significance of the current persuasive messages, which guiding behavior accordingly (see ref. 22 for review). The dmPFC, a core node in the mentalizing network, is involved in understanding others and adopting their perspectives[23], which may also facilitate attitude change[24]. However, these interpretations largely focus on static contents of persuasive information, such as the message credibility or others' perspectives. Whether the mPFC could also dynamically tracks attitude changes when exposure to evolving ambiguous and counter-attitudinal information is still unknown.

Taken together, although these previous findings have achieved a consensus that the activation of dACC and mPFC during persuasive information processing was associated with attitude changes, there are some shortcomings limit the understanding of the neural mechanisms. First, in real life, attitude change tends to unfold gradually in response to ongoing persuasive input, rather than occurring instantaneously. However, most fMRI studies have adopted event-related

designs that model attitude change as a single trial-wise event, using general linear models (GLMs) to capture transient neural responses during message presentation[1–5, 16–21]. This method treats neural fluctuations during stimulus exposure as noise[25], potentially overlooking dynamic signals that are informative for understanding how attitudes evolve. To address this limitation, inter-subject correlation (ISC) is a powerful tool for examining shared temporal neural dynamics in naturalistic contexts[26]. For instance, relevant studies captured neural dynamics while participants watched political speech, showing that greater temporal similarity in neural responses of mPFC or dACC among individuals were found when watching more persuasive videos[27,28] and for individuals with more similar pre-exist political attitudes[29–31]. This suggests that the temporal dynamics of neural responses when encoding persuasive information convey effective information related to one's attitude. However, these studies focused on pre-existing attitudes or the persuasiveness of the message, leaving the link between neural dynamics and attitude changes largely unexplored. Thus, the first goal of our study is to unfold the neural mechanism of attitude changes in naturalistic settings by focusing on the neural dynamics during persuasive information processing.

Second, attitude changes in real life are not a one-shot deal at the moment as one expected, it may evolve back and forth dynamically throughout persuasive information processing and arise spontaneously at any time. However, previous studies typically used isolated persuasive messages (e.g., health slogans or others' opinions) and asked participants to rate their attitudes before and after the short message[3–5]. This discrete, post-hoc approach to measuring attitude change fails to capture the moment-to-moment fluctuations during message exposure, and correspondingly, the attitude changes are not recorded at the precise moment the changes occurred. Thus up to now, we lack knowledge of the neural mechanism that tracks the dynamic and iterative attitude changes and also have no idea what happens in the brain at the very moment someone changes their mind. Thus, the second goal of our study is to unfold the neural mechanism that tracking the dynamic attitude changes and signaling whether and how our attitude changed at the moment it happened.

In addition, from an individual-differences perspective, attitude change can be viewed as reflecting how people cope with the uncertainty and conflict inherent in unfolding arguments. In naturalistic persuasion, individuals must continuously evaluate ambiguous, and sometimes counter-attitudinal, evidence and decide when to maintain versus revise their stance. Intolerance of uncertainty (IU) is therefore a theoretically targeted moderator, indexing stable individual differences in how people tolerate and regulate uncertainty[32]. Prior work has shown that IU shapes how individuals engage with persuasive political content, potentially because high-IU individuals show reduced openness when confronted with uncertainty[31]. Neuroimaging studies further indicate that high-IU individuals exhibit stronger activation of the dACC when processing uncertain information, highlighting dACC's role in evaluating and responding to epistemic ambiguity[33–35]. These findings raise the possibility that IU moderates dACC involvement during persuasion, potentially influencing how individuals process persuasive information and update their attitudes

in real time. Incorporating IU as a moderating variable thus provides a crucial lens for understanding individual variability in the neural mechanisms of dynamic attitude change.

To address these gaps, the current study took the advantage of naturalistic paradigm to capturing how the brain tracks dynamic, spontaneous attitude changes in naturalistic settings, and how individual traits such as IU modulate these processes. In Study 1, we aim to investigate how the neural dynamics (fluctuations over time) reflect attitude changes in naturalistic settings. Fifteen videos on different topics (Supplementary Table 1) were presented, and the time dynamics of neural responses were recorded using functional magnetic resonance imaging (fMRI). Participants were asked to report their attitudes on each topic before and after watching the video, with the difference representing attitude changes (Fig. 1A). If the temporal dynamics of neural responses can signal attitude changes, we expect that the ISC of neural responses, particularly in the mPFC and dACC, will correlate significantly with the ISC of attitude changes. In Study 2, we further enhance the naturalism of the paradigm by having participants watch a long video presenting two opposing positions on the same topic (four supporting and four opposing speakers alternated presenting their arguments, Fig. 1B; Supplementary Table 2). We allow participants to press a button whenever they perceive an attitude change. This design allows for the recording of spontaneous and dynamic attitude changes as well as the neural dynamics during persuasive information processing. If the dynamic neural responses including the regional temporal dynamics and the functional connectivity can track attitude changes in real-time, we expect that the ISC of the neural indices will correlate significantly with the ISC of attitude changes, as observed in Study 1. Moreover, at the moments when participants reported a change in their minds, we expect the neural responses at those specific moments could decode whether and how a participant has changed their mind. Additionally, how individual differences in IU modulate the neural mechanism of dynamic attitude changes were also tested. By tracking attitude change in a naturalistic setting, this research offers novel insights into how the brain dynamically integrates persuasive information to guide spontaneous and dynamic attitude changes.

Results

Descriptions of attitude changes and inter-subject similarity

In Study 1, each video elicited significant attitude changes across participants (ps < .001, Supplementary Table 3). A positive value indicated that the direction of change aligned with the persuasive stance conveyed in the video, whereas a negative value indicated that the change went against the persuasive stance (Supplementary Figure 1A). Inter-subject similarity of attitude changes was quantified by computing the inverse of the Euclidean distance between participants' attitude change vectors across the 15 topics, such that higher values reflected greater similarity in how participants changed their attitudes (Fig. 1C, see Methods for details).

In Study 2, each speaker's segment similarly induced significant attitude changes (ps < .001, Supplementary Table 3; Supplementary Figure 1B). Across the full debate, participants reported

an average of 17.11 spontaneous attitude changes, with an average interval of 174 seconds between changes (Supplementary Figure 2). To capture the dynamic trajectory of these changes, we segmented the debate into 25 consecutive 2-minute intervals and calculated directional attitude change within each segment. Inter-subject similarity was then computed using the reverse of Euclidean distance between participants across these 25 segments (Fig. 1D; see Methods for details).

The matrices and distributions of inter-subject attitude change similarity in Studies 1 and 2 are shown in Supplementary Figure 3. In addition, descriptive statistics of participants' pre-attitudes for each topic in Studies 1 and Study 2 are reported in Supplementary Table 4, showing that pre-attitudes were generally moderate (ranging from 4.97 to 9.17 on a 15-point scale). Neither the pre-attitude nor the extremity of pre-attitude was significantly associated with subsequent attitude change (*ps* > 0.1; see Supplementary Table 4 for details), suggesting that the observed attitude changes were not influenced by pre-attitude.

Shared Neural Responses During Persuasive Video Viewing

To examine whether exposure to persuasive videos elicited shared neural responses across participants[36], we computed one-to-group ISC on each region in the Schaefer200 cortical atlas[37]. Consistent with previous studies using audiovisual stimuli[29,38], ISC was highest in primary auditory and visual cortices, and was lower in motor and somatosensory regions. Moreover, in both studies, ISC was also observed in the default mode network (e.g., medial prefrontal cortex) and the executive control network (e.g., dorsolateral prefrontal cortex) (Supplementary Figure 4). These findings suggest that, regardless of whether individual attitudes changed, the persuasive videos evoked not only similar sensory processing but also shared higher-order cognitive processes related to narrative understanding[39,40].

Neural dynamics in dACC and mPFC reflect attitude changes in pre-post measurements

To identify brain regions that track attitude changes during video viewing, we employed inter-subject representational similarity analysis (IS-RSA), which links neural responses and behavioral performance by correlating inter-subject neural similarity with behavioral similarity across participant dyads[41].

In Study 1, neural similarity between each dyad was defined as the averaged ISC (Fisher z-transformed) across 15 distinct topics. To control for potential confounds, including pre-attitudes, gender, and age, we regressed these variables out from both the neural similarity matrix and the attitude change similarity matrix[42]. Pearson correlations were then computed between the residual neural and behavioral similarity matrices for 200 Schaefer parcels, and statistical significance was assessed using a Mantel test[43] (Fig. 2A, see Methods for details). IS-RSA revealed significant positive associations between neural similarity and attitude change similarity in several regions previously implicated in attitude change, including left dACC (r = 0.178, p = 0.019), left vmPFC

(r = 0.162, p = 0.050), left dmPFC (r = 0.154, p = 0.045). In addition, other regions such as the supramarginal gyrus, posterior superior and middle temporal gyri, parietal motor cortex, and visual cortex also showed significant associations (Fig. 2B, C). The brain regions showed significant results, including in the analyses without confound control, are reported in Supplementary Table 5. These results suggest that the temporal neural dynamics, particularly within the dACC and mPFC, could reflect attitude changes in naturalistic settings.

Neural dynamics in dACC activity tracks attitude changes in real-time

In Study 1, participants viewed persuasive videos presenting a single stance and reported their attitudes only before and after each video; therefore, the within-video timing of attitude changes could not be determined. To overcome this key limitation, Study 2 adopted continuous tracking, with participants reporting moment-to-moment attitudes while viewing a debate that presented conflicting perspectives. This design enabled the estimation of idiosyncratic, time-resolved trajectories of attitude change at a second-by-second timescale.

Neural similarity in Study 2 was defined as the ISC (Fisher z-transformed) of neural responses across the entire video, with potential confounds (pre-attitude, gender, and age) regressed out (see Methods for details). As in Study 1, we applied IS-RSA to relate neural and behavioral similarity for 200 Schaefer parcels. This analysis revealed a significant positive association in the left dACC (r = 0.236, p = 0.014, Mantel test; Fig. 2D, E). In contrast, no significant associations were observed in the vmPFC (r = -0.052, p = 0.345) or the dmPFC (r = 0.039, p = 0.721) (Supplementary Table 6). These findings demonstrate that the dACC, rather than the mPFC, continuously tracks how individuals adjust their attitudes in real time.

Additionally, to visualize the BOLD signal at the moments of attitude change, we time-locked each participant's dACC BOLD time series to the changing points and averaged the aligned time courses across all events. This analysis revealed a reliable increase in dACC activity, peaking 4-6 seconds after the reported attitude change (Fig. 2F), suggesting that the dACC dynamically tracks the moment participants decide to change their minds. Furthermore, to rule out the possibility that the neural similarity in dACC was driven by the increased BOLD responses at the very moments of attitude changes rather than the temporal dynamics during watching, we removed BOLD responses surrounding the attitude change events (−5 to +10 TRs), and recomputed ISC. The IS-RSA results remained significant in the left dACC (r = 0.264, p = 0.002, Mantel test; Supplementary Table 7), and the ISC before and after this exclusion were highly correlated (r = 0.832, p < 0.001). These results indicate that dACC activity tracks dynamic attitude changes throughout the viewing period, rather than being driven solely by brief responses at the moment of change.

Beyond the dACC and mPFC, additional regions such as the posterior cingulate cortex (PCC) and lateral prefrontal cortex (lPFC) also showed significant associations between neural and attitude change similarity (Supplementary Tables 6-7). However, because these regions did not

emerge in Study 1, they are not the focus of interpretation here. In addition, to address potential arbitrariness in the 2-minute segmentation approach, we repeated the analysis using a finer-grained 1-minute segmentation. The results remained consistent (Supplementary Tables 6-7), confirming the robustness of the observed neural-behavioral similarity associations.

dACC-centered dynamic inter-subject functional connectivity (dISFC) tracks attitude changes in real-time

Building on the finding that temporal dynamics in dACC activity track real-time attitude changes, we further examined whether its functional connectivity (FC) with other brain regions similarly tracks attitude changes. Using a sliding-window approach, we computed dISFC between the dACC and the other 199 cortical regions (see Methods for details). For each dACC-centered dISFC, we calculated dyadic similarity, indexing how similarly the dACC connectivity fluctuated over time while watching the video for each dyads. We then applied IS-RSA to test whether these neural similarities in dISFC were associated with behavioral attitude change similarity, after regressing out potential confounds (Fig. 3A).

The results revealed significant associations in 30 dACC-centered dISFCs, primarily involving regions within the DMN, such as the dmPFC, PCC, and precuneus (Fig. 3B, C; Supplementary Table 8). To validate whether dACC-DMN coupling specifically tracked attitude changes, we computed dISFC at the network level by averaging dACC connectivity with all parcels in each canonical network (as defined by the Schaefer atlas). Among the seven networks, only the DMN showed a significant correlation between dACC-DMN dISFC similarity and attitude change similarity ($r = 0.213$, $p = 0.015$, Mantel test), whereas no significant effects were found for other networks (Fig. 3D, Supplementary Table 9). These results extend beyond local dACC activity, demonstrating that dynamic functional interactions between the dACC and broader cortical regions, particularly the DMN, also track attitude changes in real time.

The results without controlling for the potential confounds were similar (Supplementary Table 8-9), supporting the robustness of the findings.

Dynamic attitude changes can be decoded from dACC-related neural indices

So far, we have shown that neural dynamics in the dACC and its functional connectivity, particularly with the DMN, track real-time attitude changes. Next, we tested whether these neural features could be used to decode whether and how attitude changes occurred.

First, we examined whether dACC-related neural signals during each 2-minute segment could predict the occurrence of an attitude change (Fig. 4A). For each segment, we extracted three types of neural features: (1) the average multi-voxel activity pattern of the left dACC, (2) functional connectivity (FC) between the dACC and 199 cortical regions, and (3) FC between the dACC and the DMN. A nonlinear support vector machine (SVM) classifier with leave-one-out cross-validation (LOOCV)[44] was trained using each feature type to classify Change vs. No-Change

segments. All three models achieved significant performance (Fig. 4B). Using the dACC activity pattern yielded 60.6% accuracy ($p < 0.001$; recall: 69.3% for Change, 52.5% for No-Change). The dACC-DMN FC achieved 64.9% accuracy ($p < 0.001$; recall: 62.1% for Change, 67.4% for No-Change). The dACC-centered whole-brain FC yielded the highest accuracy of 69.4% ($p < 0.001$; recall: 68.4% for Change, 70.4% for No-Change). These findings suggest that dACC activity and its functional connectivity can effectively predict whether individuals changed their attitudes during video viewing.

Second, we tested whether the direction of attitude changes could also be decoded at the moment of change. Directional changes were categorized into four classes: More Support (N = 202), More Oppose (N = 188), Less Support (N = 70), and Less Oppose (N = 83) (Fig. 4C). Given that dACC BOLD activity peaked 4-6 seconds after changes (Fig. 2F), we extracted multi-voxel patterns from the dACC at 2-3 TRs post-change and used them to train a 4-class SVM. This model failed to predict directional attitude changes (accuracy = 27.1%, $p = 0.830$). In contrast, FC features were more informative. FC between the dACC and DMN regions (computed using a 30-TR window centered on the change) yielded significant predictive accuracy (accuracy = 38.9%, $p < 0.001$; recall: 44.5% for More Support, 36.2% for More Oppose, 38.6% for Less Support, 31.3% for Less Oppose). Whole-brain dACC-centered FC further improved performance (accuracy = 46.0%, $p < 0.001$; recall: 52.5%, 46.3%, 34.3%, and 39.8% for the four categories, respectively) (Fig. 4D). The confusion matrix of LOOCV predictions and the permutation results were shown in Supplementary Figure 5.

Together, these results suggest that local dACC activity is sufficient to decode whether an attitude change occurred during a given period, whereas decoding the direction of change at the moment it occurred requires incorporating its functional interactions with other regions, particularly those within the DMN.

Intolerance of uncertainty (IU) amplifies the association between attitude change similarity and neural similarity

Lastly, we explored whether individual differences in IU modulate the association between neural similarity and attitude change similarity. Linear mixed-effects models (LMEs) were used to test the effects of attitude change similarity, joint IU (i.e., the average IU score for each dyad), and their interaction on neural similarity.

Consistent with the IS-RSA results, neural similarity in the temporal dynamics of the dACC was significantly predicted by attitude change similarity ($\beta = 0.221$, SE = 0.042, 95% CI = [0.138, 0.304], $t = 5.230$, $p < 0.001$). Moreover, the interaction between attitude change similarity and joint IU was also significant ($\beta = 0.073$, SE = 0.028, 95% CI = [0.018, 0.129], $t = 2.589$, $p = 0.010$), with the tendency that the association between attitude change similarity and neural similarity was more pronounced among individuals with higher IU (Fig. 5A-C). The main effect of joint IU was not significant ($\beta = -0.041$, SE = 0.068, 95% CI = [-0.175, 0.094], $t = -0.592$, $p = 0.555$).

Beyond temporal dynamics, we further examined whether IU moderated the relationship between attitude change similarity and neural similarity in dACC-centered dISFC with the DMN. Similarly, attitude change similarity significantly predicted dISFC similarity with the DMN (β = 0.159, SE = 0.041, 95% CI = [0.077, 0.241], t = 3.818, p < 0.0001). However, neither the interaction effect nor the main effect of joint IU reached significance at the network level (joint IU: β = -0.027, SE = 0.067, 95% CI = [-0.158, 0.103], t = -0.409, p = 0.684; interaction effect: β = 0.049, SE = 0.029, 95% CI = [-0.009, 0.106], t = 1.654, p = 0.098). To further probe potential regional effects, we tested the interaction term for each of the 30 dISFCs that were significantly associated with attitude change similarity, applying LME with FDR correction. Significant interaction effects were found for dISFCs between the dACC and several DMN-related regions, including the posterior cingulate cortex(PCC), precuneus, ventrolateral prefrontal cortex (vlPFC), left postcentral sulcus (PoCS), and left superior parietal lobule (SPL) (Supplementary Table 10). These interactions followed a similar pattern, such that higher IU amplified the relationship between neural and attitude change similarity (Fig. 5D-F).

These findings suggest that individuals who are more intolerant of uncertainty exhibit a stronger neural-behavioral coupling during attitude change. Additionally, no significant association was found between IU and pre-attitudes ($r(36)$ = -0.066, p = 0.699) , or between IU and attitude change (β = -0.019, SE = 0.055, 95% CI = [-0.126, 0.089], t = -0.339, p = 0.737).

Discussion

Given the dynamic nature of real-life attitude changes, we investigated the neural mechanisms of attitude changes in naturalistic contexts by focusing on the temporal dynamics of brain activity. We identified the dorsal anterior cingulate cortex (dACC) as a central hub in this process. Specifically, across individuals, greater similarity in attitude change trajectories during exposure to persuasive arguments was reflected in more similar temporal dynamics of dACC activity and its functional connectivity with other brain regions, particularly the DMN. These neural dynamics further predicted whether an individual changed their attitude over time, and at the precise moment of change, dACC-centered connectivity predicted the how the attitude changed. Additionally, the strength of association between dACC-related neural dynamics and attitude changes was significantly stronger in individuals with high IU. Together, these findings provide a fine-grained, dACC-centered account of the dynamic processes underlying attitude change in naturalistic settings.

A key innovation of the present study lies in emphasizing the dynamic process of attitude change in naturalistic settings. Although prior research has linked dACC activity to attitude change in contexts such as social conformity[1–5] and cognitive dissonance[6–10], these studies have typically treated attitude change as a discrete, trial-based event. Their approach captures only transient neural responses through pre-post contrasts, overlooking the gradual and temporally extended nature of attitude change. In contrast, our study demonstrated that the time-varying dynamics of

dACC activation and its functional connectivity continuously tracked attitude changes as they unfold. Notably, this relationship persisted even after excluding the BOLD signals time-locked to the exact moments when participants reported an attitude change, indicating that it is the ongoing fluctuation in dACC activity, rather than momentary spikes, that tracks attitude change. Importantly, this does not mean that the moment of change lacks neural significance. Rather, our findings show that at the precise moment of attitude change, the connectivity pattern between the dACC and the DMN predicted how participants changed their attitudes. This suggests that the dACC supports both sustained monitoring throughout the persuasive experience and transient coordination with higher-order integrative systems at critical changing moments.

After identifying the dACC as a central hub, it is time to ask what functions of dACC makes it so important? Previous interpretations of dACC function in this domain have often centered on conflict detection between internal beliefs and external input[1–5], a narrow view that fails to capture its full functional repertoire. Indeed, the dACC has been implicated in a range of processes, including conflict monitoring[45], foraging value evaluation[46], cognitive control allocation[47,48], or uncertainty processing[49]. Integrating these functions, recent computational models have proposed a broader theoretical framework in which the prefrontal cortex, including dACC, may act as a meta-reinforcement learning system—that is, learning not just what to do, but how to flexibly adapt its learning and control strategies across contexts[13,14,50]. Within this framework, individual functions serve as component processes supporting adaptive behavior: conflict monitoring flags mismatches between internal states and external input, foraging value evaluation assesses the potential benefits of switching strategies, and control allocation determines how cognitive resources are deployed to enact change. This perspective is particularly well-suited to our paradigm. Rather than responding to isolated arguments, participants engaged in a dynamic process of attitude change, i.e., interpreting incoming information in light of prior attitudes, adjusting their evaluative strategies as the narrative unfolded, and deciding when and how to revise their stance to maintain psychological coherence. From the meta-reinforcement learning standpoint, the dACC did not simply react to specific content, but acted as a higher-order "change manager", i.e., monitoring whether the ongoing flow of persuasive input destabilized current attitudes sufficiently to warrant revision, and determining both when a change should occur and how to implement it through adaptive control.

Specifically, we first found that participants with more similar trajectories of attitude change exhibited greater similarity in the neural dynamics of the dACC. This inter-subject correspondence is consistent with the possibility that attitude change relies on shared computational demands across individuals, and that dACC dynamics may contribute to meta-level monitoring of when to change one's attitude as information unfolds. Furthermore, the within-subject temporal dynamics of dACC activity predicted whether a participant changed their attitude during a given period. These findings are conceptually consistent with accounts linking dACC to foraging-like value evaluation[46], in which dACC may evaluate the relative value of persisting with the current course

of action versus shifting to an alternative, and may contribute to a threshold-like process that biases the decision to maintain or revise an existing attitude.

Second, we observed that participants who shared more similar trajectories of attitude change also demonstrated greater similarity in the dynamic functional connectivity between the dACC and the DMN. Moreover, at the moment of attitude change, the dACC-DMN coupling could predict the direction of that change, i.e., whether participants became more supportive or more opposed, depending on their initial stance. The DMN is well known for its role in integrating incoming information with internal models to construct coherent interpretations of experience[39,40,51]. In this context, dACC-DMN connectivity may reflect network-level coordination between evaluative processing and integrative interpretation during attitude change. One possibility is that increased dACC-DMN coupling marks moments when evaluation-related signals (potentially involving dACC) are more tightly coordinated with integrative representations (often associated with the DMN), facilitating the integration and re-weighting of incoming arguments, which may in turn shape the direction of attitude change at that moment.

Third, individuals with higher levels of IU exhibited stronger associations between dACC-centered neural dynamics and their attitude change behavior. Prior research in non-clinical samples has shown that individuals high in IU display heightened dACC activation and stronger connectivity with the anterior insula during uncertain decision-making and reward anticipation[52,53]. In our study, persuasive information containing ambiguous or conflicting content may have been perceived as more destabilizing by these individuals, prompting stronger recruitment of dACC-based regulatory mechanisms. IU can be regarded as a trait-level modulator of the threshold for initiating learning or control. That is, individuals with high IU possess a lower tolerance for epistemic volatility, making them more likely to engage dACC functions to evaluate whether attitude change is warranted, and leading to a stronger coupling between dACC-centered neural dynamics and observed attitude changes.

Together, these findings support a layered account of the dACC in dynamic attitude change: encoding shared belief-updating strategies, evaluating whether change is warranted, coordinating how change unfolds, and modulating this process based on individual differences in IU. Rather than mapping onto a single cognitive function, the dACC may act as a flexible hub. By situating our findings within the meta-reinforcement learning framework, we provide an integrative interpretation of how dACC dynamics could contribute to attitude change in complex, naturalistic contexts. However, the specific computational mechanisms and causal pathways underlying these effects remain to be elucidated.

Notably, our findings underscore the central role of the dACC rather than the mPFC in tracking dynamic attitude change. In Study 1, the neural dynamics of both vmPFC and dmPFC were related to attitude change assessed through pre–post measurements, suggesting that the temporal features of mPFC contribute to overall attitude changes. However, when attitude change

was measured in a more continuous and spontaneous fashion, as in Study 2, the mPFC no longer tracked these changes as robustly, whereas the dACC exhibited strong real-time tracking capabilities. The association of vmPFC and dmPFC with attitude change has been frequently reported in research on persuasive health messages (e.g., "Smoking is harmful to health"), where vmPFC activation reflects the encoding of subjective value or personal significance of the message[17,19], while the dmPFC has been implicated in understanding others' intentions or adopting others' perspectives, thereby facilitating downstream attitude change[18,24]. It seems that the mPFC may primarily contribute to attitude change by supporting integrated evaluations of argument content (e.g., value-based appraisal and mentalizing), whereas the dACC may contribute by continuously monitoring uncertainty and conflict in the unfolding information stream and signaling when updating is warranted[13,14,50]. This divergence helps explain why only the dACC but not the mPFC tracked real-time attitude changes when participants could freely decide whether and when to change their mind in response to ambiguous, unfolding arguments, rather than merely representing argument content.

It is also important to acknowledge several limitations of the present study. First, while we examined attitude change in response to persuasive input, real-life attitude change often occurs in interactive social contexts that involve reciprocal opinion exchange and negotiation toward consensus. That is, individuals do not simply integrate others' viewpoints but also express and defend their own. Recent studies using fMRI hyperscanning have shown that conversation dynamics, such as mental state alignment and topic exploration, can facilitate agreement and are associated with increased inter-brain synchrony[54]. Future research could extend our findings by examining the neural mechanisms of dynamic attitude change from a dual-brain, interactive perspective. Second, the basic unit of our analysis was the interval between two reported attitude shifts, which may span multiple persuasive arguments or rhetorical cues. It limited our ability to isolate the specific content that triggered attitude change. Recent advances in computational modeling and large language models (LLMs) have made it possible to parse naturalistic language at sentence- or even word-level granularity[55,56]. Applying such approaches could enable future studies to decode the neural signatures of attitude change with finer temporal and semantic resolution. Third, in daily life, some attitude changes reflect a "repellent" effect, where individuals' attitudes shift away from the persuasive direction. However, in our study, almost all attitude changes occurred in the direction of the persuasion. Whether attitude changes in the opposite direction share the same underlying mechanisms as those in the direction of persuasion remains an open question. Future studies could investigate this by using designs that elicit a more balanced distribution of "toward" and "away" changes to explore the neural mechanisms involved. Finally, additional moderators, including personality traits, social pressure, topic characteristics, or emotional involvement, may influence both the likelihood and trajectory of attitude change. Investigating these factors could further illuminate the boundary conditions and individual variability of the observed neural mechanisms.

In conclusion, our study highlights the dACC and its functional coupling with the DMN as central neural mechanisms supporting spontaneous and dynamic attitude change in naturalistic settings, while also acknowledging the role of individual differences in uncertainty sensitivity. By leveraging a naturalistic paradigm, we captured both the temporal evolution and the critical moments of attitude change, bridging the gap between controlled laboratory tasks and real-world social cognition. Our findings contribute to a more process-based understanding of how the brain supports dynamic attitude change, and highlight directions for future research on the temporal and neurocomputational mechanisms of attitude change in real-life contexts.

Methods

Participants

Seventy-two participants (Study1: N = 35, 15 males, mean age = 20.06±2.38 yrs; Study 2: N = 37, 16 males, mean age = 23.35±3.06 yrs) were participated in the experiments. None reported a history of psychiatric, neurological, or cognitive disorders. All participants provided written informed consent and received monetary compensation. The study was approved by the ethics committee of Northeast Normal University. All ethical regulations relevant to human research participants were followed.

Stimuli

Study 1. Fifteen videos (2-3 minutes) featuring persuasive arguments on various social issues were selected from the Chinese television program *Qi Pa Show*. Topics included marriage, career choices, morality, and hypothetical dilemmas (e.g., whether one should pursue their dreams or choose a stable job at the age of 30; see Supplementary Table 1 for details). Each video conveyed a unilateral perspective, either in support of or against the issue, without presenting competing viewpoints, ensuring clarity in the persuasive stance. Since pre-attitudes, particularly when they are extreme or strongly held, can confer greater resistance to persuasion[57], we deliberately selected topics for which public opinion was expected to be less polarized and for which both positions could be reasonably defended. This design helped ensure that participants' pre-attitudes were distributed across both sides of the scale while minimizing extreme starting positions that are typically less amenable to change.

Study 2. A single edited debate video (duration: 49'50", divided into six scans) from *Qi Pa Show* was used. The debate centered on a hypothetical question: *If a chip were implanted in the human brain, granting instant access to the entirety of human knowledge and real-time updates on new discoveries, would such a system be beneficial?* Two opposing teams, each comprising four speakers, took turns presenting their arguments and rebuttals, with each speaker contributing approximately 4 to 8 minutes of content. To fit the experimental design, irrelevant content was removed, and visual cues (e.g., audience voting results) were blurred. A detailed description of the video content is provided in the supplementary materials (Supplementary Table 2).

All stimuli used in this study are available at https://osf.io/34yrj/files/osfstorage.

Procedures

Study 1. Prior to the formal experiment, participants were given a brief overview of the 15 debate topics to ensure a baseline understanding. Following an anatomical scan, participants underwent fMRI scanning while watching the videos. The 15 videos were divided into five scans, and their order was counterbalanced across participants using a Latin square design. For each topic, the trial began with a 8-second fixation point. At the beginning of each video, the debate topic and a 15-point attitude scale were displayed at the center of the screen. Participants had 10 seconds to indicate their pre-attitude. They then watched a persuasive video presenting a one-sided argument on the topic. After the video ended, the topic and the scale were shown again for 20 seconds, and participants were asked to rate their post-video attitude. The difference between pre- and post-video ratings was taken as a measure of attitude change.

Study 2. Before the fMRI scanning, participants were introduced to the debate topic and asked to reflect on their initial opinion on a 15-point scale. The rating was later used to initialize each participant's attitude scale. After the anatomical scan, participants underwent six fMRI scans while watching the full debate video. An 8-second fixation point was presented at the beginning of each run. Throughout the video, this attitude scale remained visible on the screen, with the cursor starting at the participant's initial rating. Participants were instructed to press the left or right button to adjust the scale whenever they felt their opinion had changed, allowing real-time tracking of spontaneous attitude changes. At the end of each scan, an additional 8 seconds were provided for participants to confirm their final attitude.

In both Study 1 and Study 2, attitudes were assessed using a 15-point scale ranging from 0 ("Extremely Supportive") to 14 ("Extremely Opposed"), with 7 indicating a neutral midpoint ("Neutral"). Participants saw only the verbal anchors at the two endpoints and the midpoint. The wording of the anchors in Study 1 varied slightly depending on the specific topic, but the scale structure were identical across all measures.

After scanning, participants completed the short version of Intolerance of Uncertainty Scale[32] to assess trait-level sensitivity to uncertainty in daily life. The IU scale includes 12 items (e.g., "Unforeseen events upset me greatly"), rated on a 5-point Likert scale from 1 (not at all characteristic of me) to 5 (entirely characteristic of me).

Attitude changes and inter-subject similarity

Study 1. For each participant and each topic, attitude change was computed as the difference between the post-video and pre-video attitude ratings. To verify whether the videos reliably elicited attitude changes, we conducted one-sample t-tests on the absolute values of attitude change scores for each topic across participants. False Discovery Rate[58] (FDR) correction was applied to account for multiple comparisons.

To assess the similarity in attitude changes between participants, we calculated the Euclidean distance between each pair of participants based on their attitude change scores across the 15 topics. The Euclidean distance D between participants A and B was computed as:

$$D(A,B) = \sqrt{\sum_{i=1}^{15}(A_i - B_i)^2}$$

Where A_i and B_i denote the attitude change scores for topic i for participants A and B, respectively. To facilitate interpretation, we used the negative Euclidean distance as our similarity index, i.e., larger values indicated greater similarity between participants.

Study 2. To characterize the frequency and temporal distribution of spontaneous attitude changes, we first divided the debate video into 2-second intervals. Each interval was assigned a value of 1 if at least one attitude change occurred within it, and 0 otherwise, yielding a binary time series for each participant that marked the timing of their attitude changes (Supplementary Figure 2). Based on this temporal resolution between changes (On average, participants exhibited 17.11 attitude change points during the ~49′50″ debate video, corresponding to approximately one change every 174 seconds), we then segmented the video into 25 consecutive 2-minute intervals to capture the directional trajectory of attitude change. Because participants adjusted their ratings by moving the cursor step by step, consecutive button presses occurring within 4 seconds were treated as a single attitude change, timestamped by the first button press. For each interval, directional change was computed as the difference between the attitude ratings at the end of the segment and at the start of the segment, resulting in a 25-element vector per participant that reflected the dynamic evolution of their attitudes over time (Fig. 1D).

Inter-subject similarity in attitude change trajectories was quantified by computing the negative Euclidean distance between these 25-element vectors for each pair of participants, such that higher values indicated greater similarity. In addition to this primary analysis using 2-minute segments, we also performed a supplementary analysis dividing the video into 50 1-minute intervals, which followed the same procedure. Results based on the 2-minute segmentation are reported in the main text; results from the 1-minute segmentation are provided in Supplementary Materials (Supplementary Tables 5-6).

Additional analyses on pre-attitudes

We examined the potential influence of pre-attitudes and their extremity on attitude change in both Study 1 and Study 2. In Study 1, extremity was defined as the absolute difference between each participant's pre-attitude and the midpoint of the 15-point scale (0–14, midpoint = 7). Attitude changes were directionally coded: changes consistent with the video's persuasive direction were positive, and changes in the opposite direction were negative. For Study 2, the video was

segmented by speaker, and directional coding was applied relative to the pre-attitude at the start of each segment. Pre-attitude extremity was defined as the absolute difference between the pre-attitude and the scale midpoint for each speaker.

We used linear mixed-effects models (LMEs) with random intercepts for participants and videos (Study 1) or participants and speakers (Study 2) to test the effects of pre-attitude and pre-attitude extremity on attitude change.

fMRI Data Acquisition

MRI data were collected using a 3T GE MR750 scanner. Functional images were acquired in interleaved order using a T2*-weighted EPI sequence (32 slices, repetition time: 2 s; echo time: 30 ms; flip angle: 90°; acquisition matrix: 64; slice thickness: 4 mm^3). Anatomical images were acquired with a T1-weighted pulse sequence (TR: 8.208 ms; TE: 3.22 ms; flip angle: 12°; acquisition matrix: 256; slice thickness: 1 mm^3).

fMRI Data Preprocessing

First, raw DICOM files were converted to NIfTI format following the Brain Imaging Data Structure (BIDS) standard using HeuDiConv[59]. The first four volumes (TRs) of each functional scan were discarded to allow for magnetic field stabilization. Anatomical and functional images were then preprocessed using fMRIPrep 23.2.2[60]. Briefly, anatomical images underwent intensity non-uniformity correction, skull stripping, tissue segmentation, and normalization to MNI152NLin2009cAsym space. Functional images underwent slice timing correction, motion correction, co-registration to the anatomical image, normalization to MNI space, and resampling ($2 \times 2 \times 2\,mm^3$). Detailed preprocessing steps are provided in the Supplementary Materials (Supplementary Text).

Subsequent denoising was performed using Nilearn[61]. For each voxel, we regressed out nuisance variables including cerebrospinal fluid, white matter, global signal, six motion parameters and their first derivatives[62], as generated by fMRIPrep. Additionally, zero- and first-order polynomials were regressed out to remove linear trends, followed by high-pass filtering (cutoff = 0.008 Hz). Then, spatial smoothing (Gaussian kernel, FWHM = 6 mm) was applied for univariate analyses, while multivoxel pattern analyses (MVPA) were conducted on unsmoothed data. The residual BOLD time series were standardized (z-scored within scan) for concatenation across scans and used for further statistical analysis.

To ensure data quality, framewise displacement[63] (FD) was computed using motion parameters estimated by fMRIPrep. Participants with mean FD > 0.5 mm should be excluded[64]. All participants in Study 1 and Study 2 had mean FD values below this threshold, with average FD of 0.10 mm and 0.11 mm, respectively.

Atlas and ROI definitions

We extracted time series of the the BOLD signals for each parcel in the Schaefer 200-parcel cortical atlas[37] (200 parcels, 7-network version; www.templateflow.org). The atlas is based on a functional connectivity-driven clustering of resting-state fMRI data, providing a standardized parcellation of the cerebral cortex into 200 spatially contiguous parcels assigned to seven large-scale functional networks: Default Mode Network (DMN), Control Network, Salience/Ventral Attention Network (VAN), Somatomotor, Visual, Limbic, and Dorsal Attention Network (DAN).

In our main analyses, the dorsal anterior cingulate cortex (dACC) corresponds to parcel #90, labeled 7Networks_LH_Default_PFC_8; the dorsomedial prefrontal cortex (dmPFC) corresponds to parcel #84, labeled 7Networks_LH_Default_PFC_2; and ventromedial prefrontal cortex (vmPFC) corresponds to parcel #92, labeled 7Networks_LH_Default_PFC_10.

Averaged one-to-group ISC on the neural responses across participants

To quantify the consistency of time-resolved neural responses elicited by the video stimuli, we performed an ISC analysis[38]. Specifically, for each participant, we extracted time series of the the BOLD signals for each parcel and concatenated the z-scored BOLD signals across scans. Notably, only BOLD signals during video viewing were retained, while pre- and post-rating periods were excluded. One-to-group ISC was then computed by correlating each participant's parcel-wise time series with the average time series of all other participants. The resulting Pearson correlation coefficients were averaged across participants to generate a map of inter-subject similarity in neural responses (Supplementary Figure 4).

To determine statistical significance of the parcel-wise ISC, we conducted a permutation test. Specifically, for each parcel, the signs of ISC values were randomly flipped across participants, and t-statistics were recomputed across 10,000 permutations to construct a null distribution. Two-tailed p-values were obtained by counting how often the permuted statistics exceeded or equaled the absolute value of the observed statistic, with both numerator and denominator incremented by 1 to avoid zero p-values. This approach followed that of Leong et al.[29].

Calculation of dyad-level inter-subject similarity of neural indices

Temporal dynamics of single brain regions. In Study 1, dyad-level ISC was calculated for each video by correlating parcel-wise BOLD time series between participant pairs. Pearson correlation coefficients were Fisher z-transformed and averaged across the 15 topics, providing an overall measure of neural similarity across topics. In Study 2, neural signals across six scans were concatenated and then used to compute dyad-level ISC, yielding a measure of inter-subject neural similarity throughout the full debate.

Dynamic inter-subject functional connectivity (dISFC). After identifying dACC time series that tracked attitude change, we examined whether the dynamic coupling of dACC with the remaining 199 regions also predicted attitude changes in Study 2. One-to-group dISFC was computed using a sliding-window approach (window size = 30 TRs, step = 1 TR)[65,66]. For each

region and each window, we calculated the Pearson correlation between each participant's dACC time series and the average time series of another brain region across all other participants. The correlations were Fisher z-transformed, yielding 199 dACC-centered dISFC time series per participant, each containing 1,464 time points. We then computed the similarity of dISFC time series between participant dyads for each region using Pearson correlation.

Since a substantial number of dISFCs were found to be associated with attitude change, we further computed dISFC at the network level (as defined by the Schaefer atlas[37]), we averaged dISFC values between the dACC and all parcels within that network. For example, dynamic dACC-DMN connectivity was calculated by averaging across dACC's functional connectivity with 45 DMN parcels (excluding dACC). This yielded network-level time series of dISFC between dACC and each brain network.

Control Analyses

To control for potential confounding variables, including similarity in pre-attitudes, gender, and age, we regressed out these variables from both the inter-subject similarity of attitude change and the neural similarity indices (i.e., temporal dynamics of single regions, regional-level dISFC, and network-level dISFC). Specifically, pre-attitude similarity was quantified as the Euclidean distance between participants' initial ratings, gender similarity was coded as a binary variable indicating whether the pair shared the same gender, and age difference was computed as the absolute difference in age. The residuals from these regressions were then used in the subsequent IS-RSA with Mantel tests. All the results reported in the main text were based on this confound-controlled data. Results without controlling for these variables are reported in the Supplementary Materials (Supplementary Tables 4-8).

Inter-Subject Representational Similarity Analysis (IS-RSA)

We used inter-subject representational similarity analysis[41] (IS-RSA) to identify brain regions where neural similarity aligned with similarity in attitude change. Specifically, standardized dyad-level neural similarities, derived from regional temporal dynamic, regional-level dISFC, and network-level dISFC, were used to construct neural similarity matrices. Correspondingly, a behavioral similarity matrix was generated based on the Euclidean distances between participants' attitude change trajectories (Fig. 2A, Fig. 3A). For each neural index, we computed the Pearson correlation between the upper triangles of the neural and behavioral similarity matrices. Higher correlation coefficients indicate a stronger correspondence between neural dynamics and behavioral attitude changes.

To account for dyadic non-independence, we performed a Mantel permutation test (N = 10,000 times) to assess the statistic significance of the association between the neural similarity and attitude change similarity. At each time, participant identities were randomly permuted by applying the same random shuffle to both the rows and columns of the neural similarity matrix,

thereby maintaining its symmetry while disrupting the correspondence between neural and behavioral similarities. We then recalculated the correlation between matrices to build a null distribution[39,42]. Statistical significance was determined using a two-tailed p-value.

Decoding dynamic attitude changes from dACC-related neural indices

First, To predict whether an individual changed their attitude within a given period, we conducted a binary classification analysis on 2-minute segments of the debate video (~50 minutes total) from Study 2. A total of 925 segments were contributed by 37 participants. Each segment was labeled as either "Change" (N = 449) or "No-Change" (N = 476), depending on whether an attitude change occurred during that time window. For each segment, we extracted three types of neural features: (1) The average multivoxel activation pattern in the left dACC (644 voxels; 60 TRs), (2) Functional connectivity (FC) between the dACC and all the other regions in the whole brain (199 regions), and (3) FC between the dACC and DMN (45 regions). The FC was computed as the Pearson correlation between the time series of each region pair over the full segment duration (60 TRs). These three feature sets were used respectively to train classifiers to predict whether an attitude change occurred.

Next, we aimed to decode the direction of attitude change at the precise moments when participants changed their attitudes. Each attitude change was categorized based on the pre-attitude and the direction of change, resulting in four labels: More Support (N = 202), More Oppose (N = 188), Less Support (N = 70), and Less Oppose (N = 83). Changes from neutral to support or from neutral to oppose were excluded. To predict these labels, we again extracted three types of neural features: (1) Multivoxel activation patterns in the left dACC (644 voxels), averaged over the 2nd and 3rd TRs following the moment of change, based on the observed BOLD peak latency in this region, (2) FC between the dACC and the other 199 cortical regions, and (3) FC between the dACC and DMN regions. The FC features were calculated within a 30-TR (60 s) window centered on the moment of change (15 TRs before to 14 TRs after), balancing temporal resolution and estimation stability, following previous work[65,66].

Classification was performed using a nonlinear support vector machine (SVM) with leave-one-out cross-validation (LOOCV) implemented in scikit-learn[44]. To address class imbalance, we applied the “balanced” option in SVM, which adjusts class weights inversely proportional to class frequencies in the training set. LOOCV ensured that each participant served once as the test subject, enabling an unbiased estimation of model performance. To evaluate statistical significance, we conducted a permutation test by repeating the entire classification procedure 1,000 times with randomly shuffled labels in the training folds. This generated a null distribution of LOOCV accuracies under the assumption of no relationship between neural features and behavioral labels. A two-tailed p-value was computed based on the proportion of permutations exceeding the observed accuracy.

Moderation effects of intolerance of uncertainty (IU)

We used linear mixed effects models (LMEs) to test whether IU moderates the relationship between neural similarity and attitude change similarity. Neural similarity served as the dependent variable, while the similarity in attitude change was treated as a predictor. The average IU score for each participant pair (i.e., joint IU)[30] was included as a moderator. Moderation analyses were restricted to neural features that significantly tracked attitude change in prior IS-RSA results, namely the dACC time series, dACC-DMN dISFC and dACC-centered regional-level dISFCs. All variables were standardized before model fitting. Two random intercepts were specified to account for the non-independence of dyadic data[30,67]. The model was specified as follows:

$$\mathrm{NS}_{ij} = \beta_0 + \beta_1 \cdot \mathrm{IU}_{ij} + \beta_2 \cdot \mathrm{BS}_{ij} + \beta_3 \cdot \left(\mathrm{IU}_{ij} \times \mathrm{BS}_{ij}\right) + u_i + u_j + \epsilon_{ij}$$

Where NS_{ij} is the neural similarity for participants i and j; IU_{ij} is the joint IU (moderating variable) for participants i and j; BS_{ij} is the attitude change similarity for participants i and j; The β_1, β_2, and β_3 are the coefficients for joint IU, attitude change similarity, and their interaction, respectively. The u_i and u_j are the random intercepts for participants i and j. The ϵ_{ij} is the residual error term. All models were estimated using the Python package pymer4[68].

Additionally, we examined whether IU was related to participants' pre-attitudes and subsequent attitude change. Pearson correlation was used to test the association between IU and pre-attitudes. Given that attitude change involves repeated measures for each participant, we calculated directional attitude change (defined relative to the persuasive direction) for each speaker and each participant. A linear mixed-effects model (LME) with random intercepts for participants and speakers was then used to test whether IU influenced attitude change.

Statistics and reproducibility

The sample size was determined with reference to previous studies in the field. Neuroimaging data were preprocessed using fMRIPrep (version 23.2.2) and further denoised with Nilearn (version 0.12.1). All statistical analyses were conducted in Python 3 (version 3.12.2). To assess the relationship between behavioral and neural similarity, we performed Inter-Subject Representational Similarity Analysis (IS-RSA) using custom-written code with 10,000 permutation tests. To examine the moderating effect of intolerance of uncertainty, we employed Linear Mixed Effects (LME) models implemented with the pymer4 package (version 0.8.4) and applied FDR-BH correction for multiple comparisons. Decoding analyses were conducted using scikit-learn (version 1.7.1). All results were considered significant if the p-value was less than 0.05.

Reporting summary

Further information on research design is available in the Nature Portfolio Reporting Summary linked to this article.

Data availability

The studies were not preregistered. Raw neuroimaging data are publicly available on OpenNeuro (Study 1: https://openneuro.org/datasets/ds006559[69]; Study 2: https://openneuro.org/datasets/ds006568[70]). Preprocessed neural data, behavioral data and video stimuli are available on OSF (https://osf.io/34yrj/files/osfstorage).

Code availability

Codes used to reproduce the analyses and figures are available on Github (https://github.com/Llihaiming/dynamic-attitude-change.git).

Author contributions

Haiming Li and Yi Liu conceived the study. Bing Wu provided access to experimental facilities. Haiming Li, Senmu Yao and Bing Wu collected the data. Haiming Li and Yu Zhang developed the experimental materials and analyzed the data. Haiming Li wrote the first draft of the manuscript. Yi Liu revised the manuscript.

Competing interests

The authors declare no competing interests.

References

1. Berns, G. S., Capra, C. M., Moore, S. & Noussair, C. Neural mechanisms of the influence of popularity on adolescent ratings of music. *NeuroImage* **49**, 2687–2696 (2010).
2. Campbell-Meiklejohn, D. K., Bach, D. R., Roepstorff, A., Dolan, R. J. & Frith, C. D. How the Opinion of Others Affects Our Valuation of Objects. *Curr. Biol.* **20**, 1165–1170 (2010).
3. Klucharev, V., Hytönen, K., Rijpkema, M., Smidts, A. & Fernández, G. Reinforcement Learning Signal Predicts Social Conformity. *Neuron* **61**, 140–151 (2009).
4. Mahmoodi, A., Nili, H., Bang, D., Mehring, C. & Bahrami, B. Distinct neurocomputational mechanisms support informational and socially normative conformity. *PLOS Biol.* **20**, e3001565 (2022).
5. Zaki, J., Schirmer, J. & Mitchell, J. P. Social Influence Modulates the Neural Computation of Value. *Psychol. Sci.* **22**, 894–900 (2011).
6. Van Veen, V., Krug, M. K., Schooler, J. W. & Carter, C. S. Neural activity predicts attitude change in cognitive dissonance. *Nat. Neurosci.* **12**, 1469–1474 (2009).
7. Izuma, K. *et al.* Neural correlates of cognitive dissonance and choice-induced preference change. *Proc. Natl. Acad. Sci.* **107**, 22014–22019 (2010).
8. Izuma, K. & Adolphs, R. Social Manipulation of Preference in the Human Brain. *Neuron* **78**, 563–573 (2013).
9. Izuma, K. *et al.* A Causal Role for Posterior Medial Frontal Cortex in Choice-Induced Preference Change. *J. Neurosci.* **35**, 3598–3606 (2015).
10. Kitayama, S., Chua, H. F., Tompson, S. & Han, S. Neural mechanisms of dissonance: An fMRI investigation of choice justification. *NeuroImage* **69**, 206–212 (2013).
11. Izuma, K. The neural basis of social influence and attitude change. *Curr. Opin. Neurobiol.* **23**, 456–462 (2013).
12. Wu, H., Luo, Y. & Feng, C. Neural signatures of social conformity: A coordinate-based activation likelihood estimation meta-analysis of functional brain imaging studies. *Neurosci. Biobehav. Rev.* **71**, 101–111 (2016).
13. Wang, J. X. *et al.* Prefrontal cortex as a meta-reinforcement learning system. *Nat. Neurosci.* **21**, 860–868 (2018).
14. Silvetti, M., Vassena, E., Abrahamse, E. & Verguts, T. Dorsal anterior cingulate-brainstem ensemble as a reinforcement meta-learner. *PLOS Comput. Biol.* **14**, e1006370 (2018).
15. Eckstein, M. K., Wilbrecht, L. & Collins, A. G. What do reinforcement learning models measure? Interpreting model parameters in cognition and neuroscience. *Curr. Opin. Behav. Sci.* **41**, 128–137 (2021).
16. Doré, B. P., Cooper, N., Scholz, C., O'Donnell, M. B. & Falk, E. B. Cognitive regulation of ventromedial prefrontal activity evokes lasting change in the perceived self-relevance of persuasive messaging. *Hum. Brain Mapp.* **40**, 2571–2580 (2019).

17. Chua, H. F., Liberzon, I., Welsh, R. C. & Strecher, V. J. Neural Correlates of Message Tailoring and Self-Relatedness in Smoking Cessation Programming. *Biol. Psychiatry* **65**, 165–168 (2009).
18. Wang, A.-L. *et al.* Content Matters: Neuroimaging Investigation of Brain and Behavioral Impact of Televised Anti-Tobacco Public Service Announcements. *J. Neurosci.* **33**, 7420–7427 (2013).
19. Falk, E. B. *et al.* Self-affirmation alters the brain's response to health messages and subsequent behavior change. *Proc. Natl. Acad. Sci.* **112**, 1977–1982 (2015).
20. Falk, E. B., Berkman, E. T., Mann, T., Harrison, B. & Lieberman, M. D. Predicting Persuasion-Induced Behavior Change from the Brain. *J. Neurosci.* **30**, 8421–8424 (2010).
21. Vezich, I. S., Katzman, P. L., Ames, D. L., Falk, E. B. & Lieberman, M. D. Modulating the neural bases of persuasion: why/how, gain/loss, and users/non-users. *Soc. Cogn. Affect. Neurosci.* **12**, 283–297 (2017).
22. Falk, E. & Scholz, C. Persuasion, Influence, and Value: Perspectives from Communication and Social Neuroscience. *Annu. Rev. Psychol.* **69**, 329–356 (2018).
23. Amodio, D. M. & Frith, C. D. Meeting of minds: the medial frontal cortex and social cognition. *Nat. Rev. Neurosci.* **7**, 268–277 (2006).
24. Welborn, B. L. *et al.* Neural mechanisms of social influence in adolescence. *Soc. Cogn. Affect. Neurosci.* **11**, 100–109 (2016).
25. Ben-Yakov, A., Honey, C. J., Lerner, Y. & Hasson, U. Loss of reliable temporal structure in event-related averaging of naturalistic stimuli. *NeuroImage* **63**, 501–506 (2012).
26. Ntoumanis, I. *et al.* Deciphering the neural responses to a naturalistic persuasive message. *Proc. Natl. Acad. Sci.* **121**, e2401317121 (2024).
27. Imhof, M. A., Schmälzle, R., Renner, B. & Schupp, H. T. Strong health messages increase audience brain coupling. *NeuroImage* **216**, 116527 (2020).
28. Imhof, M. A., Schmälzle, R., Renner, B. & Schupp, H. T. How real-life health messages engage our brains: Shared processing of effective anti-alcohol videos. *Soc. Cogn. Affect. Neurosci.* **12**, 1188–1196 (2017).
29. Leong, Y. C., Chen, J., Willer, R. & Zaki, J. Conservative and liberal attitudes drive polarized neural responses to political content. *Proc. Natl. Acad. Sci.* **117**, 27731–27739 (2020).
30. Van Baar, J. M., Halpern, D. J. & FeldmanHall, O. Intolerance of uncertainty modulates brain-to-brain synchrony during politically polarized perception. *Proc. Natl. Acad. Sci.* **118**, e2022491118 (2021).
31. De Bruin, D., Van Baar, J. M., Rodríguez, P. L. & FeldmanHall, O. Shared neural representations and temporal segmentation of political content predict ideological similarity. *Sci. Adv.* **9**, eabq5920 (2023).
32. Carleton, R. N., Norton, M. A. P. J. & Asmundson, G. J. G. Fearing the unknown: A short version of the Intolerance of Uncertainty Scale. *J. Anxiety Disord.* **21**, 105–117 (2007).

33. Krain, A. L. *et al.* A Functional Magnetic Resonance Imaging Investigation of Uncertainty in Adolescents with Anxiety Disorders. *Biol. Psychiatry* **63**, 563–568 (2008).
34. Krain, A. L. *et al.* An fMRI examination of developmental differences in the neural correlates of uncertainty and decision-making. *J. Child Psychol. Psychiatry* **47**, 1023–1030 (2006).
35. Morriss, J., Bell, T., Biagi, N., Johnstone, T. & Van Reekum, C. M. Intolerance of uncertainty is associated with heightened responding in the prefrontal cortex during cue-signalled uncertainty of threat. *Cogn. Affect. Behav. Neurosci.* **22**, 88–98 (2022).
36. Nastase, S. A., Gazzola, V., Hasson, U. & Keysers, C. Measuring shared responses across subjects using intersubject correlation. *Soc. Cogn. Affect. Neurosci.* **14**, 667–685 (2019).
37. Schaefer, A. *et al.* Local-Global Parcellation of the Human Cerebral Cortex from Intrinsic Functional Connectivity MRI. *Cereb. Cortex* **28**, 3095–3114 (2018).
38. Hasson, U., Nir, Y., Levy, I., Fuhrmann, G. & Malach, R. Intersubject Synchronization of Cortical Activity During Natural Vision. *Science* **303**, 1634–1640 (2004).
39. Nguyen, M., Vanderwal, T. & Hasson, U. Shared understanding of narratives is correlated with shared neural responses. *NeuroImage* **184**, 161–170 (2019).
40. Yeshurun, Y., Nguyen, M. & Hasson, U. The default mode network: where the idiosyncratic self meets the shared social world. *Nat. Rev. Neurosci.* **22**, 181–192 (2021).
41. Finn, E. S. *et al.* Idiosynchrony: From shared responses to individual differences during naturalistic neuroimaging. *NeuroImage* **215**, 116828 (2020).
42. Iyer, S., Collier, E., Broom, T. W., Finn, E. S. & Meyer, M. L. Individuals who see the good in the bad engage distinctive default network coordination during post-encoding rest. *Proc. Natl. Acad. Sci.* **121**, e2306295121 (2024).
43. Chen, G. *et al.* Untangling the relatedness among correlations, part I: Nonparametric approaches to inter-subject correlation analysis at the group level. *NeuroImage* **142**, 248–259 (2016).
44. Pedregosa, F. *et al.* Scikit-learn: Machine Learning in Python. *J. Mach. Learn. Res.* https://inria.hal.science/hal-00650905 (2011).
45. Botvinick, M. M., Braver, T. S., Barch, D. M., Carter, C. S. & Cohen, J. D. Conflict monitoring and cognitive control. *Psychol. Rev.* **108**, 624–652 (2001).
46. Kolling, N., Behrens, T. E. J., Mars, R. B. & Rushworth, M. F. S. Neural Mechanisms of Foraging. *Science* **336**, 95–98 (2012).
47. Shenhav, A., Botvinick, M. M. & Cohen, J. D. The Expected Value of Control: An Integrative Theory of Anterior Cingulate Cortex Function. *Neuron* **79**, 217–240 (2013).
48. Shenhav, A., Cohen, J. D. & Botvinick, M. M. Dorsal anterior cingulate cortex and the value of control. *Nat. Neurosci.* **19**, 1286–1291 (2016).
49. Tomov, M. S., Truong, V. Q., Hundia, R. A. & Gershman, S. J. Dissociable neural correlates of uncertainty underlie different exploration strategies. *Nat. Commun.* **11**, 2371 (2020).

50. Vriens, T., Vassena, E., Pezzulo, G., Baldassarre, G. & Silvetti, M. Meta-Reinforcement Learning reconciles surprise, value, and control in the anterior cingulate cortex. *PLOS Comput. Biol.* **21**, e1013025 (2025).
51. Simony, E. *et al.* Dynamic reconfiguration of the default mode network during narrative comprehension. *Nat. Commun.* **7**, 12141 (2016).
52. Radoman, M. & Gorka, S. M. Intolerance of uncertainty and functional connectivity of the anterior insula during anticipation of unpredictable reward. *Int. J. Psychophysiol.* **183**, 1–8 (2023).
53. DeSerisy, M., Musial, A., Comer, J. S. & Roy, A. K. Functional connectivity of the anterior insula associated with intolerance of uncertainty in youth. *Cogn. Affect. Behav. Neurosci.* **20**, 493–502 (2020).
54. Speer, S. P. H. *et al.* Finding Agreement: fMRI hyperscanning reveals dyads that explore in mental state space facilitate opinion alignment. 2024.10.03.616501 Preprint at https://doi.org/10.1101/2024.10.03.616501 (2025).
55. Heilbron, M., Armeni, K., Schoffelen, J.-M., Hagoort, P. & de Lange, F. P. A hierarchy of linguistic predictions during natural language comprehension. *Proc. Natl. Acad. Sci.* **119**, e2201968119 (2022).
56. Zada, Z. *et al.* A shared model-based linguistic space for transmitting our thoughts from brain to brain in natural conversations. *Neuron* **112**, 3211-3222.e5 (2024).
57. Howe, L. C. & Krosnick, J. A. Attitude Strength. *Annu. Rev. Psychol.* **68**, 327–351 (2017).
58. Benjamini, Y. & Hochberg, Y. Controlling the False Discovery Rate: A Practical and Powerful Approach to Multiple Testing. *J. R. Stat. Soc. Ser. B Methodol.* **57**, 289–300 (1995).
59. Halchenko, Y. O. *et al.* HeuDiConv — flexible DICOM conversion into structured directory layouts. *J. Open Source Softw.* **9**, 5839 (2024).
60. Esteban, O. *et al.* fMRIPrep: a robust preprocessing pipeline for functional MRI. *Nat. Methods* **16**, 111–116 (2019).
61. Abraham, A. *et al.* Machine learning for neuroimaging with scikit-learn. *Front. Neuroinformatics* **8**, (2014).
62. Friston, K. J., Williams, S., Howard, R., Frackowiak, R. S. J. & Turner, R. Movement-Related effects in fMRI time-series. *Magn. Reson. Med.* **35**, 346–355 (1996).
63. Power, J. D., Barnes, K. A., Snyder, A. Z., Schlaggar, B. L. & Petersen, S. E. Spurious but systematic correlations in functional connectivity MRI networks arise from subject motion. *NeuroImage* **59**, 2142–2154 (2012).
64. Power, J. D., Schlaggar, B. L. & Petersen, S. E. Recent progress and outstanding issues in motion correction in resting state fMRI. *NeuroImage* **105**, 536–551 (2015).
65. Song, H., Finn, E. S. & Rosenberg, M. D. Neural signatures of attentional engagement during narratives and its consequences for event memory. *Proc. Natl. Acad. Sci.* **118**, e2021905118 (2021).
66. Song, H., Park, B., Park, H. & Shim, W. M. Cognitive and Neural State Dynamics of Narrative Comprehension. *J. Neurosci.* **41**, 8972–8990 (2021).

67. Chen, G., Taylor, P. A., Shin, Y.-W., Reynolds, R. C. & Cox, R. W. Untangling the relatedness among correlations, Part II: Inter-subject correlation group analysis through linear mixed-effects modeling. *NeuroImage* **147**, 825–840 (2017).
68. Jolly, E. Pymer4: Connecting R and Python for Linear Mixed Modeling. *J. Open Source Softw.* **3**, 862 (2018).
69. Attitude Change Study 1 Persuade Dateset. *OpenNeuro* https://doi.org/10.18112/openneuro.ds006559.v1.0.0 (2025).
70. Attitude Change Study 2 Debate Dateset. *OpenNeuro* https://doi.org/10.18112/openneuro.ds006568.v1.0.0 (2025).

Figure captions

Fig. 1 | Experimental Design. A Participants watched 15 videos on different social issues while undergoing fMRI. Before and after each video, they rated their attitudes toward each issue on a 15-point scale. The list of topics, stances, and video durations are provided in Supplementary Table 1. **B** Participants watched a ~50-minute debate video and continuously reported their attitudes in real time on a 15-point scale while undergoing fMRI. The duration of each speaker's segment, their stances, main arguments and the fMRI run structure are provided in Supplementary Table 2. **C** Attitude change was calculated as post-rating minus pre-rating, and these changes were aligned across participants by topic. **D** The debate was divided into 25 consecutive two-minute segments, and participants' attitude change was calculated for each segment. Similarities in attitude change across the two studies were computed as the inverse of the Euclidean distance between their attitude change vectors.

Fig. 2 | Results of ISC in single brain regions. **A** Illustration of the IS-RSA pipeline. For each parcel, pairwise neural similarity was computed using Pearson correlations on the times series of BOLD signals. The association between the neural similarity and behavioral similarity was assessed using IS-RSA with 10,000 permutations. **B-C** Brain regions showed significant association between neural similarity and attitude change similarity in Study 1. Significance was assessed using two-tailed permutation tests (**$p < 0.01$, *$p < 0.05$). Brain regions are labeled according to the Schaefer atlas (See Supplementary Table 5 for details). **D** Brain regions showed significant association between neural similarity and attitude change similarity in Study 2. **E** Positive association between neural similarity in the left dACC and attitude change similarity. **F** Averaged BOLD signals (solid line) in the dACC from all participants and all attitude change events. The blue shaded area indicates the standard error of the mean. The gray dashed line represents the onset of attitude change.

Fig. 3 | Results of dISFC. A Illustration of IS-RSA based on dISFC. Time-varying dACC-centered connectivity was computed using a sliding-window approach, where each participant's dACC time series was correlated with the averaged time series of each other brain region across all other participants. This produced pairwise matrices of inter-subject dISFC similarity for each connection. IS-RSA was then applied to examine the relationship between similarity in dACC-centered connectivity dynamics and similarity in attitude-change trajectories. **B** Cortical surface maps showing brain regions where dACC-centered dISFC similarity was significantly associated with similarity in attitude change. **C** Circular barplot of significant regions identified by IS-RSA. Bar heights represent correlation values (r), and colors indicate network identity (see Supplementary Table 8 for details). **D** Bar plot showing network-level IS-RSA results. Significance was assessed using two-tailed permutation tests. n.s. represents not significant.

Fig. 4 | Decoding attitude change from neural data in Study 2. A The debate video (~50 min) was divided into 2-minute segments. Each segment for each participant was labeled as Change or No-Change depending on whether an attitude change occurred, resulting in a total of 925 segments. **B** Classification results for predicting segment-wise attitude change (panel A) using three types of neural features during each 2-minute segments.

Accuracy was estimated using leave-one-out cross-validation, and p-values were computed via permutation tests. The blue dashed line indicates chance level (50%). **C** Each instance of attitude change was categorized into four labels based on the pre-attitude and the direction of change: More Support, More Oppose, Less Support, and Less Oppose. **D** Classification results for predicting the direction of attitude change using three types of neural features around the moment of attitude change. Accuracy was estimated using leave-one-subject-out cross-validation, and p-values were computed via permutation tests. The blue dashed line indicates chance level (25%).

Fig. 5 | Modulating role of intolerance of uncertainty (IU). A The association between dACC neural similarity and attitude change similarity is moderated by IU; higher joint IU amplifies this relationship. All variables were standardized prior to analysis. **B** Simulated neural similarity based on the regression model in panel A. **C** Marginal effects of neural similarity on attitude change similarity at low (First quartile, Q1; blue) and high (Third quartile, Q3; red) levels of joint IU, derived from panel A. **D** Brain regions where the similarity of dISFC with dACC was associated with attitude similarity and was significantly moderated by IU. These include the bilateral precuneus, right posterior cingulate cortex (PCC), left ventrolateral prefrontal cortex (vlPFC), left postcentral sulcus (PoCS), and left superior parietal lobule (SPL) (Supplementary Table 10). **E** Estimated effect of IU on dISFC similarity between left dACC and left precuneus. **F** Marginal effects of IU on dACC–precuneus dISFC at low (First quartile, Q1; blue) and high (Third quartile, Q3; red) levels of joint IU.

Editorial Summary:
Naturalistic fMRI reveals that dynamic attitude change is tracked and driven by dorsal anterior cingulate cortex activity and its connectivity with the default mode network, with intolerance of uncertainty modulating these neural–behavioral dynamics.

Peer Review Information:
Communications Biology thanks Christoph Korn and the other, anonymous, reviewer(s) for their contribution to the peer review of this work. Primary Handling Editor: Jasmine Pan. A peer review file is available.

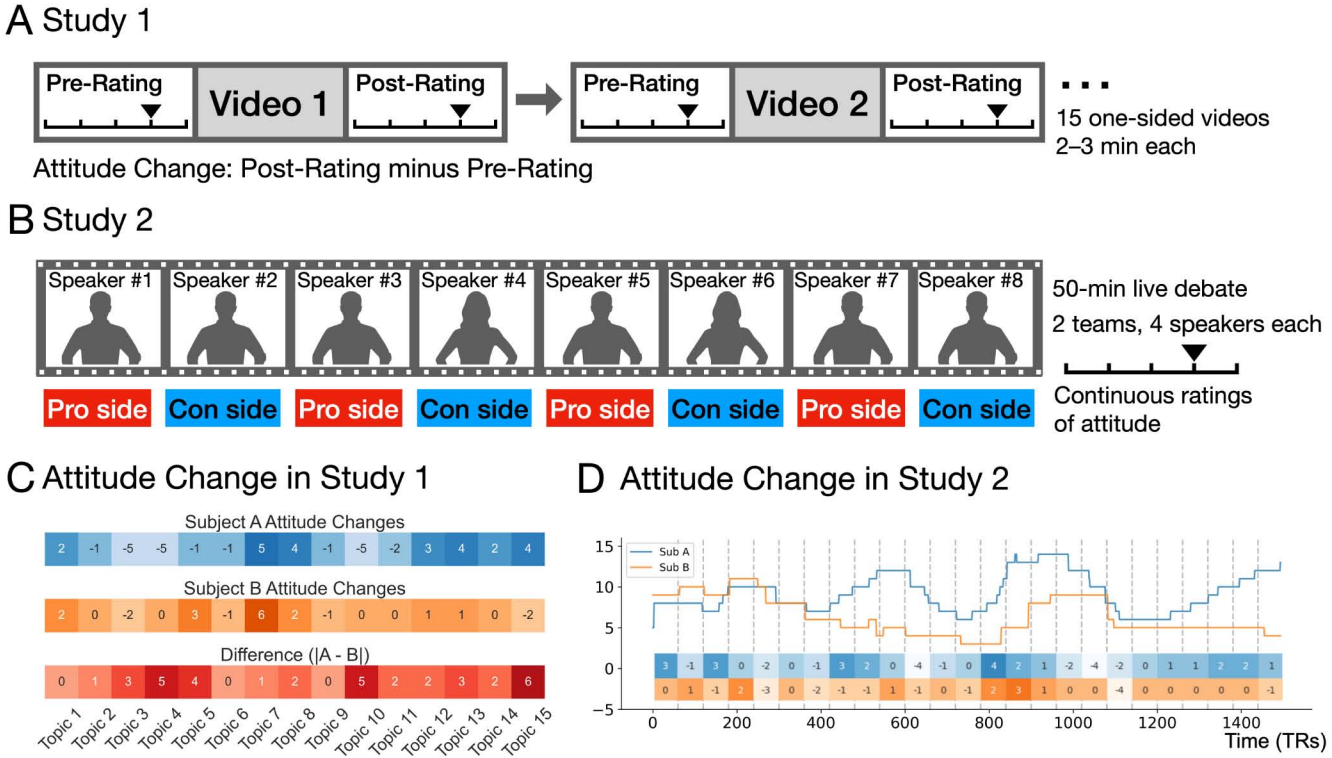
A Study 1
Pre-Rating
Video 1
Post-Rating
Pre-Rating
Video 2
Post-Rating
15 one-sided videos
2–3 min each
Attitude Change: Post-Rating minus Pre-Rating
B Study 2
Speaker #1
Speaker #2
Speaker #3
Speaker #4
Speaker #5
Speaker #6
Speaker #7
Speaker #8
Pro side
Con side
Pro side
Con side
Pro side
Con side
Pro side
Con side
50-min live debate
2 teams, 4 speakers each
Continuous ratings
of attitude
C Attitude Change in Study 1
Subject A Attitude Changes
Subject B Attitude Changes
Difference (|A - B|)
Topic 1
Topic 2
Topic 3
Topic 4
Topic 5
Topic 6
Topic 7
Topic 8
Topic 9
Topic 10
Topic 11
Topic 12
Topic 13
Topic 14
Topic 15
D Attitude Change in Study 2
Sub A
Sub B
Time (TRs)

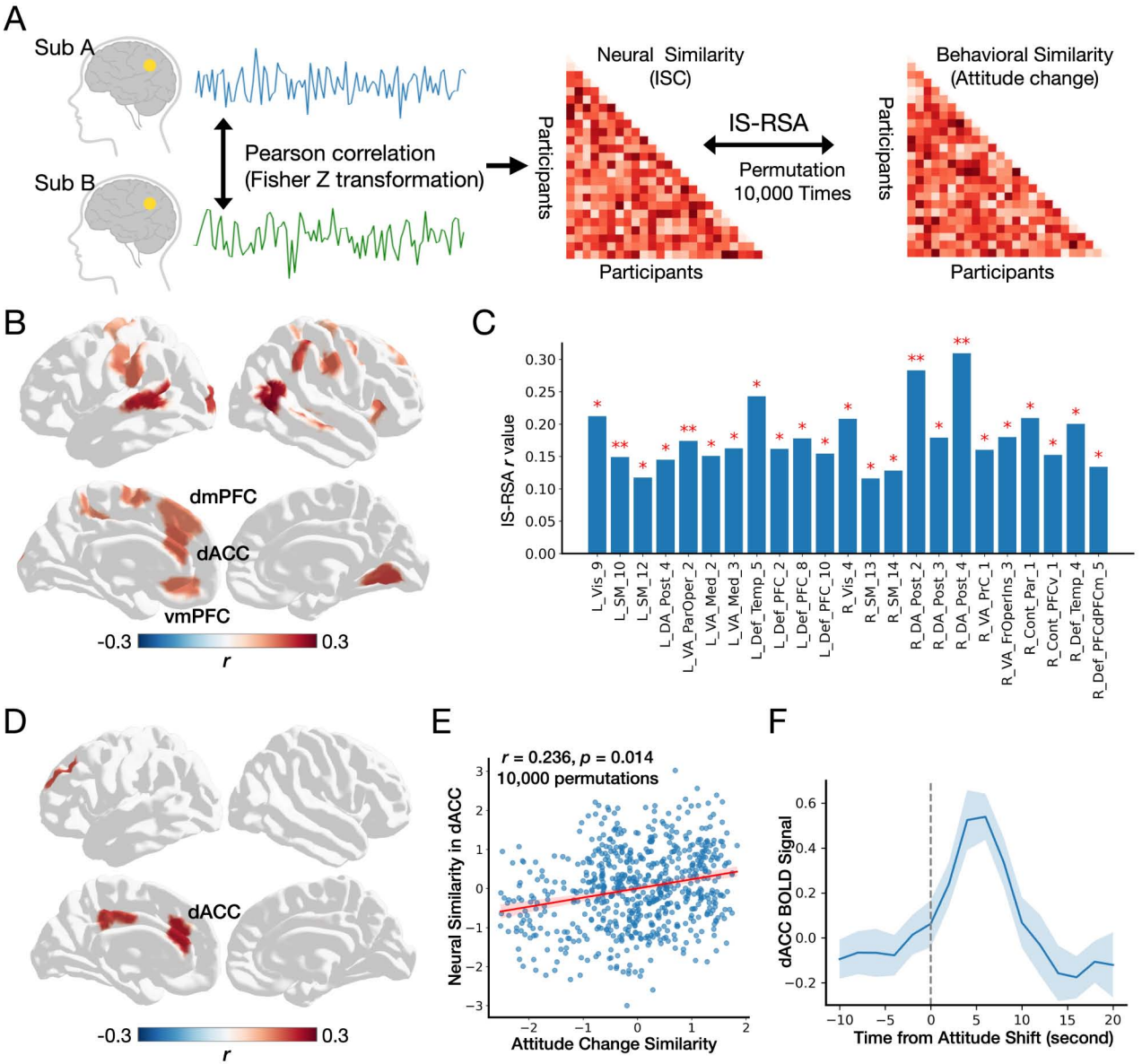
A
Sub A
Sub B
Pearson correlation
(Fisher Z transformation)
Neural Similarity
(ISC)
Participants
Participants
IS-RSA
Permutation
10,000 Times
Behavioral Similarity
(Attitude change)
Participants
Participants
B
dmPFC
dACC
vmPFC
-0.3
0.3
r
C
IS-RSA r value
0.30
0.25
0.20
0.15
0.10
0.05
0.00
L_Vis_9
L_SM_10
L_SM_12
L_DA_Post_4
L_VA_ParOper_2
L_VA_Med_2
L_VA_Med_3
L_Def_Temp_5
L_Def_PFC_2
L_Def_PFC_8
L_Def_PFC_10
R_Vis_4
R_SM_13
R_SM_14
R_DA_Post_2
R_DA_Post_3
R_DA_Post_4
R_VA_PrC_1
R_VA_FrOperIns_3
R_Cont_Par_1
R_Cont_PFCv_1
R_Def_Temp_4
R_Def_PFCdPFCm_5
D
dACC
-0.3
0.3
r
E
r = 0.236, p = 0.014
10,000 permutations
Neural Similarity in dACC
Attitude Change Similarity
F
dACC BOLD Signal
Time from Attitude Shift (second)

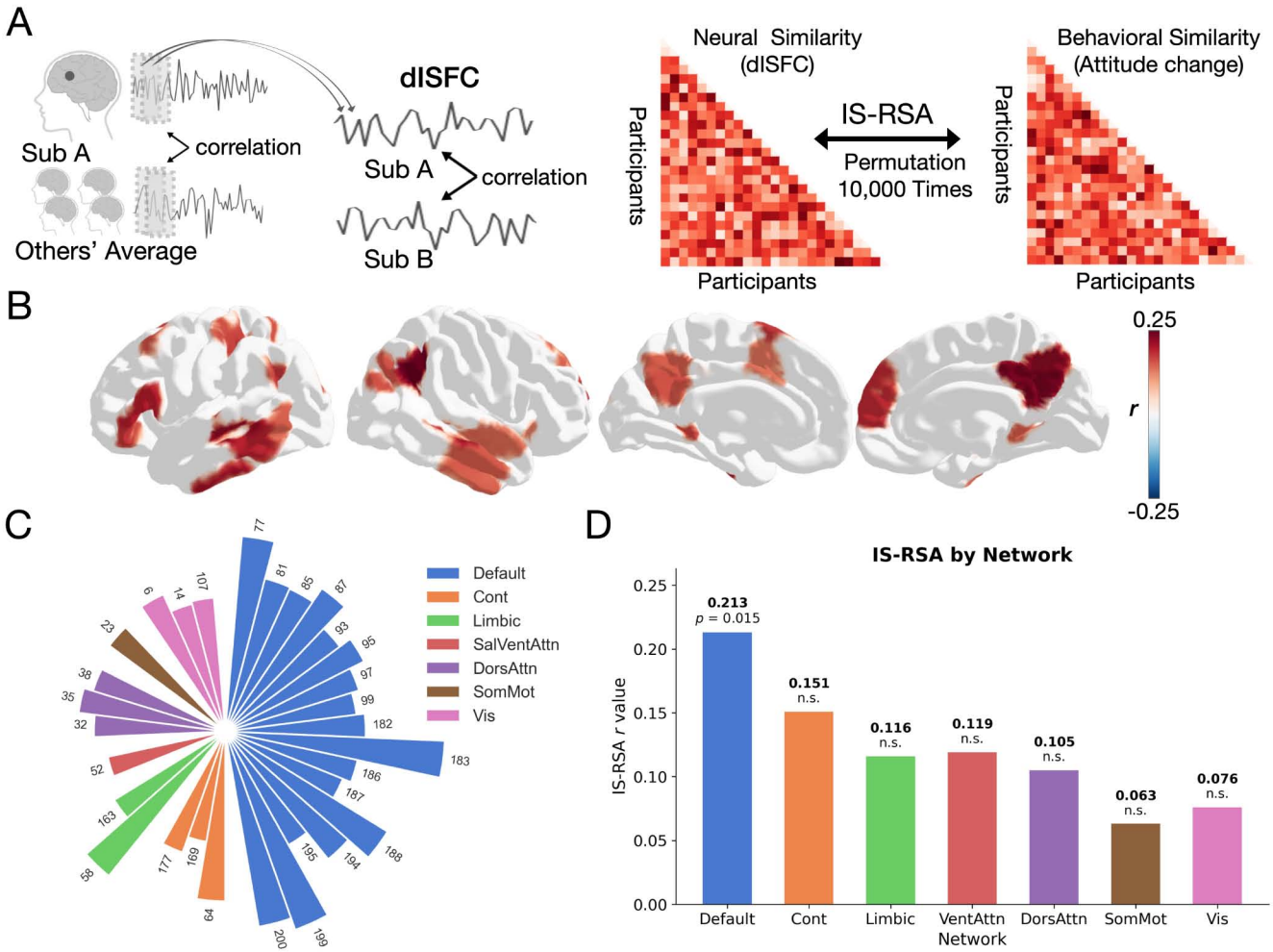
A
Sub A
correlation
Others' Average
dISFC
Sub A
correlation
Sub B
Neural Similarity
(dISFC)
Participants
Participants
IS-RSA
Permutation
10,000 Times
Behavioral Similarity
(Attitude change)
Participants
Participants
B
0.25
r
-0.25
C
Default
Cont
Limbic
SalVentAttn
DorsAttn
SomMot
Vis
77
81
85
87
93
95
97
99
182
183
186
187
188
194
195
200
199
64
169
177
58
163
52
32
35
38
23
6
14
107
D
IS-RSA by Network
IS-RSA r value
0.25
0.20
0.15
0.10
0.05
0.00
0.213
p = 0.015
0.151
n.s.
0.116
n.s.
0.119
n.s.
0.105
n.s.
0.063
n.s.
0.076
n.s.
Default
Cont
Limbic
VentAttn
DorsAttn
SomMot
Vis
Network

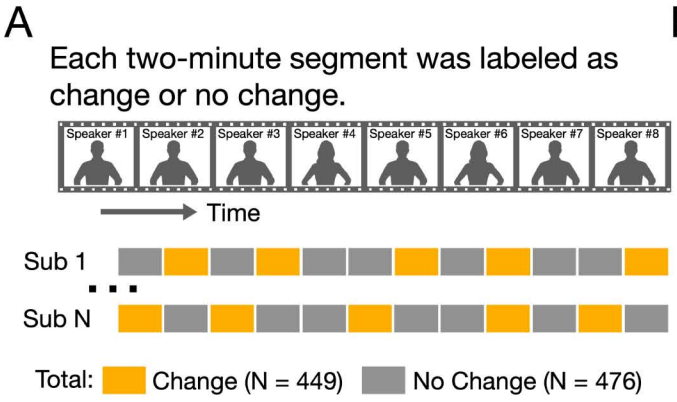
A
Each two-minute segment was labeled as change or no change.
Speaker #1
Speaker #2
Speaker #3
Speaker #4
Speaker #5
Speaker #6
Speaker #7
Speaker #8
Time
Sub 1
Sub N
Total:
Change (N = 449)
No Change (N = 476)

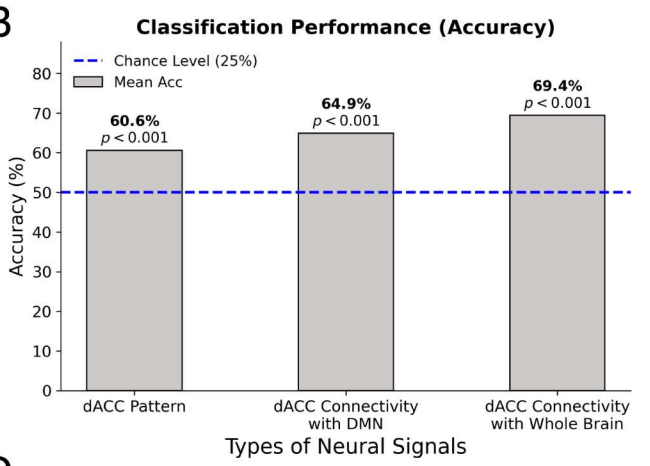
B
Classification Performance (Accuracy)
Chance Level (25%)
Mean Acc
60.6%
p < 0.001
64.9%
p < 0.001
69.4%
p < 0.001
Accuracy (%)
dACC Pattern
dACC Connectivity with DMN
dACC Connectivity with Whole Brain
Types of Neural Signals

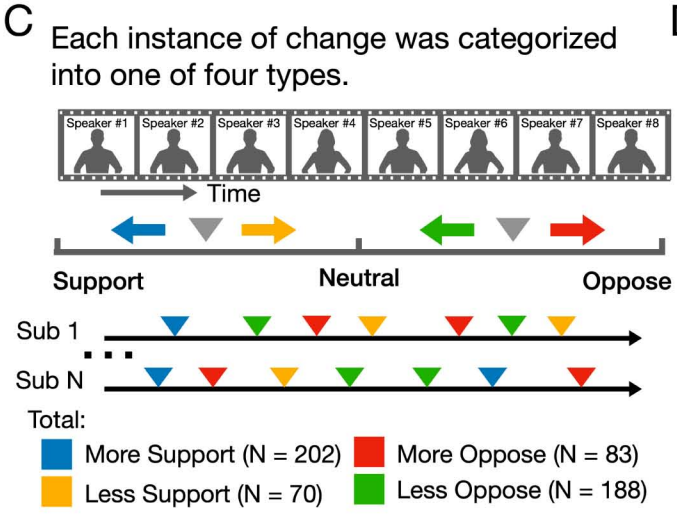
C
Each instance of change was categorized into one of four types.
Speaker #1
Speaker #2
Speaker #3
Speaker #4
Speaker #5
Speaker #6
Speaker #7
Speaker #8
Time
Support
Neutral
Oppose
Sub 1
Sub N
Total:
More Support (N = 202)
More Oppose (N = 83)
Less Support (N = 70)
Less Oppose (N = 188)

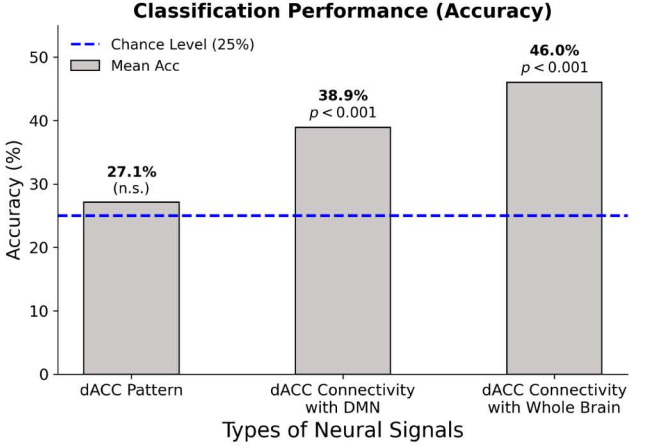
D
Classification Performance (Accuracy)
Chance Level (25%)
Mean Acc
27.1%
(n.s.)
38.9%
p < 0.001
46.0%
p < 0.001
Accuracy (%)
dACC Pattern
dACC Connectivity with DMN
dACC Connectivity with Whole Brain
Types of Neural Signals

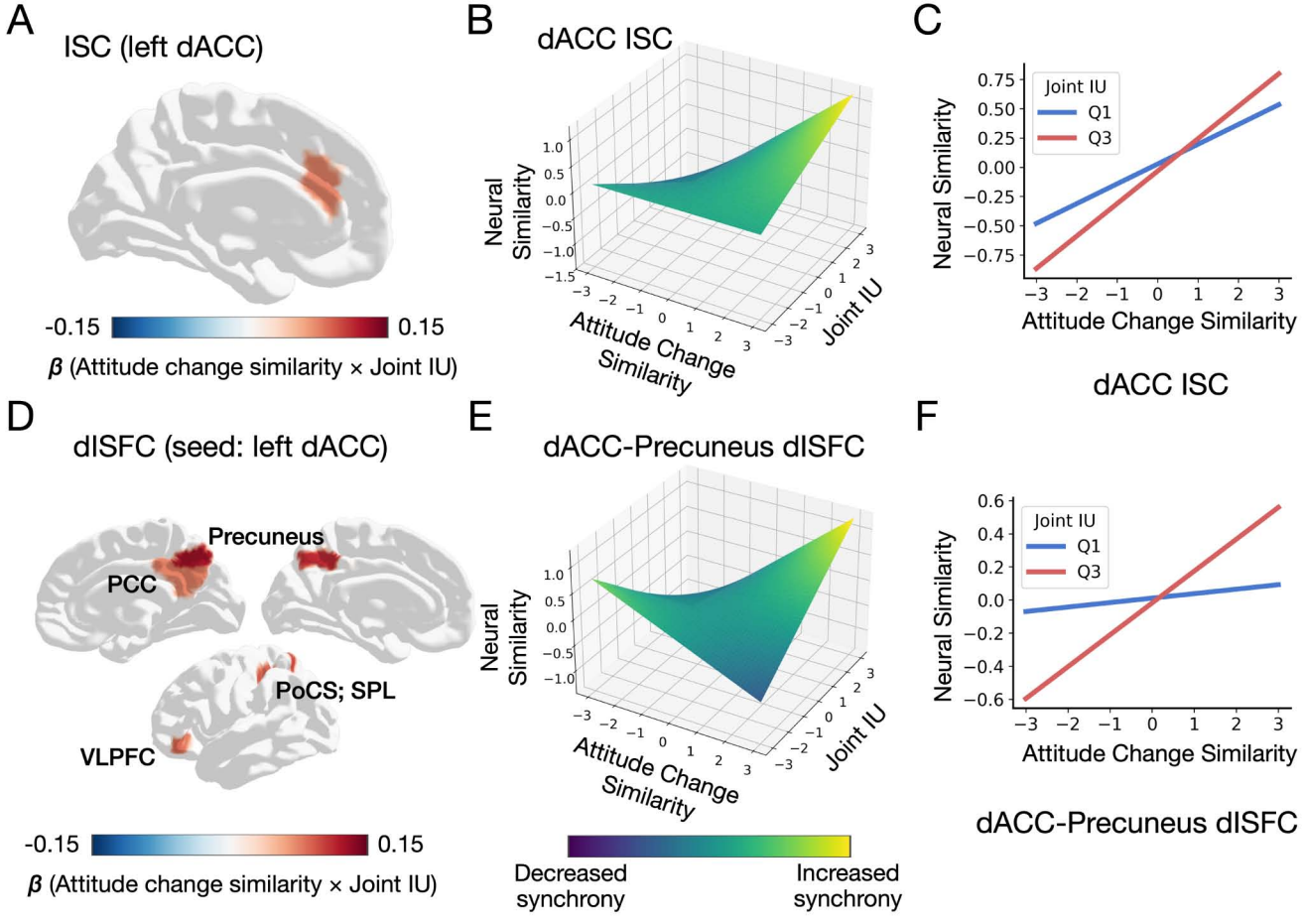
A
ISC (left dACC)
-0.15
0.15
β (Attitude change similarity × Joint IU)
B
dACC ISC
Neural Similarity
Attitude Change Similarity
Joint IU
C
Joint IU
Q1
Q3
Neural Similarity
Attitude Change Similarity
dACC ISC
D
dISFC (seed: left dACC)
Precuneus
PCC
PoCS; SPL
VLPFC
-0.15
0.15
β (Attitude change similarity × Joint IU)
E
dACC-Precuneus dISFC
Neural Similarity
Attitude Change Similarity
Joint IU
Decreased synchrony
Increased synchrony
F
Joint IU
Q1
Q3
Neural Similarity
Attitude Change Similarity
dACC-Precuneus dISFC